https://doi.org/10.5194/wes-2026-200
Preprint. Discussion started: 13 November 2026
© Author(s) 2026. CC BY 4.0 License.



eawe european academy of wind energy
Open Access WIND ENERGY SCIENCE DISCUSSIONS

Boundary-Layer Regimes and Wind Energy Climate Resilience in North Africa: A Comparative Assessment of Egypt and Morocco

Yousry Saad Badry[1]
[1] Department of Natural Resources (Meteorology), Faculty of African Postgraduate Studies, Cairo University, 12613 Giza, Egypt
Correspondence to: Yousry Saad Badry (Yousry.Saad.Badry@faps.cu.edu.eg)
Initial: Y.S. Badry

Abstract

Egypt and Morocco have Africa's most ambitious wind energy programs, yet the climate resilience of their wind resources remains poorly constrained by conventional approaches that overlook fundamental atmospheric processes. Here we introduce a boundary-layer regime framework that classifies wind farm sites according to their dominant wind-generation mechanism—Mechanically Forced (M-BL), Thermally Forced (T-BL), or Complex Forced (C-BL)—and apply it to twelve wind farms across Egypt's Gulf of Suez and Morocco's Atlantic and Mediterranean coasts. Using a consistent CORDEX-Africa CMIP5 ensemble under RCP 8.5 through 2100, combined with validated baseline wind power density from ERA5 reanalysis, we analyze projected changes using the delta change method. We find a hierarchy of climate vulnerability governed by boundary-layer physics. Egyptian M-BL sites and Moroccan southern M-BL sites show the greatest resilience (mean $\Delta WPD_{50} = +1.6\%$), while Moroccan T-BL sites (Essaouira, Taza) and C-BL sites (Tanger I, II) show larger declines (mean $\Delta WPD_{50} = -5.5\%$ and -10.8%, respectively). The Mediterranean SST corridor creates a shared threat with divergent outcomes: Tanger remains viable because topographic acceleration at the Strait of Gibraltar partially compensates for the weakened thermal gradient, whereas the Egyptian Mediterranean coast has no wind farms because it lacks such compensation. The Zafarana case shows that urbanization can override M-BL resilience. The regime hierarchy is consistent with a companion CMIP6-based analysis, suggesting that the framework is robust to scenario-generation and ensemble-size differences. Our framework provides a physics-based, universally applicable tool for climate risk assessment in wind energy development.

Keywords: boundary layer; wind energy; climate resilience; Egypt; Morocco; CORDEX-Africa; CMIP5; Mediterranean SST

1. Introduction

Wind energy is central to global decarbonization, with installed capacity reaching 837 GW by 2022 and offsetting approximately 1.2 billion tonnes of CO_2 annually (GWEC, 2022). This rapid expansion, however, rests on an implicit assumption: that the wind resource itself will remain stable over the 20–30year lifetime of a wind farm. That assumption is increasingly untenable. The atmospheric dynamics that generate and sustain near-surface winds are being altered by the same warming that wind power seeks to mitigate (Pryor and Barthelmie, 2010; Pryor et al., 2020). Robust projections of how wind resources will evolve are therefore essential for protecting the multi-billion-dollar investments that underpin the energy transition, particularly in regions where wind energy deployment is accelerating most rapidly.

North Africa presents a critical testbed for this challenge. Egypt and Morocco have emerged as continental leaders in wind energy, with installed capacities of 1,635 MW and 1,220 MW respectively, and national targets of 14% and 52% renewable electricity by 2035 (NREA, 2022; Usman and Amegroud, 2019). Both countries possess world-class wind resources: the Gulf of Suez in Egypt, driven by the persistent Etesian winds, and the Atlantic coast of Morocco, influenced by the Canary Current trade wind system and complex topographic interactions (Mortensen et al., 2006; Nfaoui et al., 1998). Yet the climate resilience of these resources remains poorly constrained. Most wind energy climate projections rely on downscaled General Circulation Model output that resolves synoptic-scale circulation but fails to capture the boundary-layer processes that govern wind generation at turbine hub heights (Tobin et al., 2016).

https://doi.org/10.5194/wes-2026-200
Preprint. Discussion started: 13 November 2026
© Author(s) 2026. CC BY 4.0 License.



eawe european academy of wind energy
Open Access WIND ENERGY SCIENCE DISCUSSIONS

The planetary boundary layer mediates the transfer of momentum, heat, and moisture between the surface and the free atmosphere (Stull, 1988), and the mechanisms that generate and sustain wind within this layer—large-scale pressure gradients, local thermal contrasts, and topographic acceleration—confer fundamentally different sensitivities to a warming climate (Petersen et al., 1998a, b). A predictive framework that incorporates these first-order physical controls has remained elusive.

We propose a boundary-layer regime classification that categorizes wind farm sites according to their dominant wind-generation mechanism: Mechanically Forced (M-BL), Thermally Forced (T-BL), or Complex Forced (C-BL). The central hypothesis is that regime membership predicts climate sensitivity. M-BL sites, anchored in large-scale circulation, should prove relatively robust to warming. T-BL sites, dependent on local temperature gradients, should be highly vulnerable because warming directly weakens the thermal contrasts that drive their winds. C-BL sites, where multiple mechanisms interact, should exhibit intermediate or context-dependent sensitivity (Atkinson, 1981; Whiteman, 2000).

The Egyptian Mediterranean coast provides a critical negative control for this hypothesis. Despite the 2006 Egyptian Wind Atlas identifying this coast as having an "excellent wind regime" reaching 7 m s^{-1} (Mortensen et al., 2006), no wind park operates there today (Tonbol et al., 2024). Recent assessments indicate that wind speeds along the coast are dominated by the 4–6 m s^{-1} range, an order of magnitude below the 8–11 m s^{-1} observed in the Gulf of Suez (Tonbol et al., 2024). This coast is influenced by Mediterranean SST gradients and land–sea thermal contrasts—a T-BL regime—rather than the topographically channeled Etesian flow that dominates the Gulf of Suez. The Etesian wind system has weakened since 1980 (Gandham et al., 2025), suggesting that the Mediterranean coast's thermal regime is becoming even less favorable for wind energy development. This contrast—one coast with world-class wind farms, the other with none—is a natural experiment in boundary-layer regime control of wind energy viability.

This study makes three contributions. First, we apply the boundary-layer regime framework to twelve wind farms in Egypt and Morocco, using a consistent CORDEX-Africa CMIP5 ensemble. Second, we compare the climate resilience of the two national portfolios, showing that Egypt's M-BL-dominated resource is more resilient than Morocco's mixed portfolio. Third, we use the Egyptian Mediterranean coast as a negative control to demonstrate that regime membership, not geography alone, determines wind energy viability. The SST-driven mechanism of northern Moroccan vulnerability is analyzed in detail in a companion study (Badry et al., under review) and is not repeated here. Section 2 presents the theoretical framework. Section 3 describes the study areas, data, and methods. Section 4 presents results. Section 5 discusses the physical mechanisms, compares with previous studies, and derives policy implications. Section 6 concludes.

---

2. Theoretical Framework

2.1 Defining Boundary-Layer Regimes

The atmospheric boundary layer (ABL) is the portion of the troposphere directly influenced by the Earth's surface, responding to surface forcing on timescales of an hour or less (Stull, 1988). Within this layer, the wind field is shaped by a superposition of forcing mechanisms that operate across a wide range of spatial and temporal scales (Lehner and Rotach, 2018; Farina and Zardi, 2023). Over complex terrain, these mechanisms include orographic gravity waves, thermally driven circulations, turbulent mixing, and synoptic-scale pressure gradients (Kirshbaum et al., 2018). We propose a three-category classification scheme based on the first-order physical process that dominates wind generation at turbine hub height (80–150 m).

Mechanically Forced Boundary Layer (M-BL). Winds are driven primarily by large-scale, persistent pressure gradients associated with synoptic weather systems. The energy source is regional to global in scale. The boundary

https://doi.org/10.5194/wes-2026-200
Preprint. Discussion started: 13 November 2026
© Author(s) 2026. CC BY 4.0 License.



eawe european academy of wind energy
Open Access WIND ENERGY SCIENCE DISCUSSIONS

layer typically exhibits near-neutral stability, efficient vertical momentum mixing, and low sensitivity to local surface heating. Examples include the trade wind systems that persist over subtropical oceans (Petersen et al., 1998a).

Thermally Forced Boundary Layer (T-BL). Winds are generated by local temperature contrasts that create density-driven flows, including sea breezes, land breezes, mountain–valley winds, and slope flows. The energy source is local and diurnally varying, leading to pronounced cycles in boundary-layer stability (Atkinson, 1981; Whiteman, 2000). These regimes are directly coupled to surface temperature gradients: warming alters the very thermal contrasts that power the circulation.

Complex Forced Boundary Layer (C-BL). Multiple forcing mechanisms interact, often intensified by topographic acceleration. Large-scale synoptic flows are modified, channeled, or accelerated by complex terrain features such as straits, mountain gaps, and irregular coastlines (Kirshbaum et al., 2018). The Strait of Gibraltar jet, where Atlantic northwesterlies are funneled and accelerated through a narrow gap, exemplifies this regime (Dorman et al., 1995).

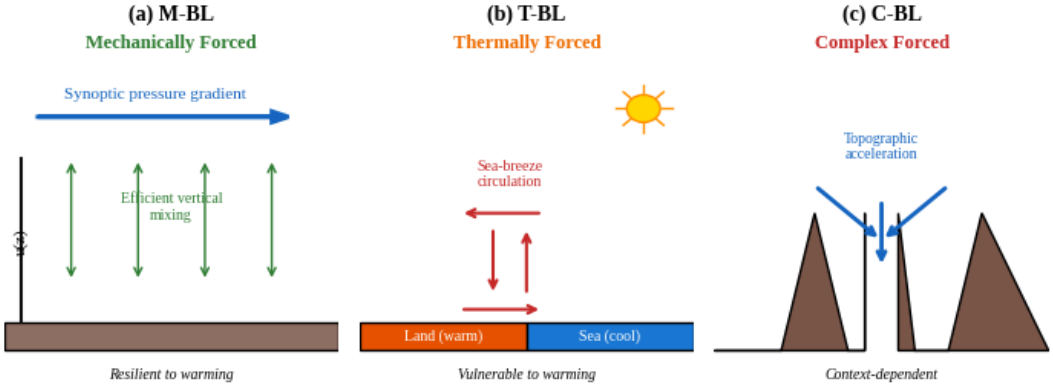


Figure 1. *Schematic of the three boundary-layer regimes showing dominant forcing mechanisms and expected climate sensitivity. (a) Mechanically Forced (M-BL), anchored in large-scale circulation. (b) Thermally Forced (T-BL), dependent on local temperature contrasts. (c) Complex Forced (C-BL), where topographic acceleration interacts with synoptic and thermal forcing.*

Table 1. *Boundary-layer regime classification and theoretical climate sensitivity.*

BL Regime	Primary forcing mechanism	Key characteristics	Expected climate resilience
Mechanical (M-BL)	Large-scale pressure gradients	Near-neutral stability; low diurnal variability; efficient vertical mixing	High—anchored in robust large-scale circulation
Thermal (T-BL)	Local temperature contrasts	Strong diurnal cycles; stability varies; direct coupling to surface heating	Low—warming weakens thermal gradients
Complex (C-BL)	Topographic acceleration + synoptic + thermal	High spatial variability; site-specific interactions	Moderate to low—context-dependent

https://doi.org/10.5194/wes-2026-200
Preprint. Discussion started: 13 November 2026
© Author(s) 2026. CC BY 4.0 License.



eawe european academy of wind energy
Open Access WIND ENERGY SCIENCE DISCUSSIONS

2.2 Link to Wind Energy Metrics and Hypotheses

Each BL regime has distinct implications for wind energy resources and their response to climate change. For M-BL sites, wind resource quality is determined primarily by the strength and persistence of the large-scale pressure gradient. Climate warming may alter this gradient through changes in synoptic patterns, but the direct thermodynamic effect of local warming is minimal (Pryor et al., 2020). For T-BL sites, the wind resource is directly coupled to surface temperature contrasts. Warming increases atmospheric stability, which suppresses vertical momentum transfer and can weaken thermally driven flows (Miller et al., 2003). For C-BL sites, the response depends on the balance of forces and the sensitivity of topographic acceleration to changes in upstream flow characteristics and static stability (Lionello and Scarascia, 2018; Dorman et al., 1995).

We define climate resilience as the ability of a wind resource to maintain its power-generating potential under long-term climate change, operationalized through percentage changes in wind power density (ΔWPD%). The central hypothesis is that BL regime membership predicts climate resilience: M-BL sites will show the smallest declines, T-BL sites the largest declines, and C-BL sites intermediate or context-dependent responses.

---

3. Study Areas and Methods

3.1 Study Areas

This study compares wind energy resources at twelve sites across two North African countries: six wind farms along Egypt's Gulf of Suez and six wind farms along Morocco's Atlantic and Mediterranean coasts. All sites are analyzed using the same CORDEX-Africa CMIP5 ensemble and the same methodology.

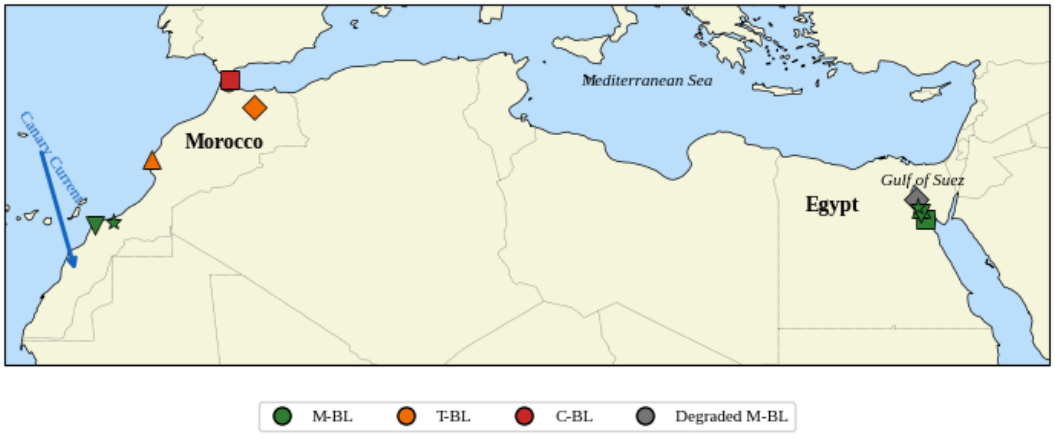


Figure 2. *Map of the study area showing Egyptian and Moroccan wind farm sites, color-coded by boundary-layer regime (M-BL, green; T-BL, orange; C-BL, red; degraded M-BL, grey). The Mediterranean SST corridor is indicated. The Canary Current is shown with a blue arrow.*
Note: Map created by the author using Cartopy and Natural Earth data (public domain).

Egypt — Gulf of Suez. Six wind farm sites were selected along Egypt's Gulf of Suez (Table 2). The Gulf of Suez is a narrow, fault-bounded basin-oriented northwest–southeast, flanked by the Red Sea mountains to the west and the Sinai massif to the east. The basin acts as a topographic channel that accelerates the prevailing north-northwest Etesian

https://doi.org/10.5194/wes-2026-200
Preprint. Discussion started: 13 November 2026
© Author(s) 2026. CC BY 4.0 License.



eawe european academy of wind energy
Open Access WIND ENERGY SCIENCE DISCUSSIONS

winds, producing one of the highest-quality wind resources in the Middle East and North Africa region (Mortensen et al., 2006). All six sites are classified a priori as M-BL. Zafarana is treated as a separate case: its observed 10 m wind speed has declined by approximately 1 m s^{-1} over recent decades, attributed to urbanization and increased surface roughness (Khalfallah and Koliub, 2007). This non-climatic override of M-BL resilience is analyzed in Section 4.4.

Table 2. *Egyptian wind farm sites.*

Site	Latitude (°N)	Longitude (°E)	Capacity (MW)	Status	BL Regime
Gabel El-Zeit	28.06	33.24	580	Operational	M-BL
Ras Ghareb	28.11	33.15	262.5	Operational	M-BL
West Bakr	28.67	32.84	252	Operational	M-BL
Zafarana	29.19	32.60	545	Operational	M-BL (degraded)
Gulf of Suez I	28.43	32.90	250	Under construction	M-BL
Gulf of Suez II	28.73	32.75	501.7	Under construction	M-BL

Morocco — Atlantic and Mediterranean Coasts. Six wind farm sites were selected in Morocco, spanning three BL regimes (Table 3). The C-BL sites (Tanger I and Tanger II) are located at the Strait of Gibraltar, where Atlantic northwesterlies are funneled and accelerated through a narrow gap (Dorman et al., 1995). The Mediterranean SST gradient plays a role in modulating the pressure field across the strait (Badry et al., under review). The T-BL sites comprise Essaouira, dominated by sea-breeze circulations (Miller et al., 2003), and Taza, located in the corridor between the Rif and Middle Atlas mountains where diurnal mountain–valley circulations dominate (Whiteman, 2000). The M-BL sites (Tarfaya and Akhfener) are dominated by the persistent Canary Current trade winds (McGregor et al., 2018).

Table 3. *Moroccan wind farm sites.*

Site	Latitude (°N)	Longitude (°W)	Capacity (MW)	Region	BL Regime
Tanger I	35.65	5.61	140	North	C-BL
Tanger II	35.82	5.45	140	North	C-BL
Essaouira	31.39	9.80	60.35	Central	T-BL
Taza	34.27	4.12	86.4	Inland	T-BL

https://doi.org/10.5194/wes-2026-200
Preprint. Discussion started: 13 November 2026
© Author(s) 2026. CC BY 4.0 License.



eawe european academy of wind energy
Open Access WIND ENERGY SCIENCE DISCUSSIONS

Site	Latitude (°N)	Longitude (°W)	Capacity (MW)	Region	BL Regime
Tarfaya	27.72	12.95	301.3	South	M-BL
Akhfener	27.95	11.98	197.7	South	M-BL

The Mediterranean SST Corridor. The northern coast of Morocco (Tanger I, Tanger II) and the Egyptian Mediterranean coast share a common atmospheric influence: the Mediterranean Sea. Both are located within the Mediterranean SST corridor, where sea surface temperatures warm approximately 20% faster than the global ocean average (Lionello and Scarascia, 2018). However, the two locations differ in topography. The Tanger sites are situated at the Strait of Gibraltar, where Atlantic northwesterlies are funneled and accelerated, creating a topographically enhanced C-BL regime. The Egyptian Mediterranean coast lacks such topographic acceleration and is dominated by T-BL thermal forcing. Recent assessments indicate that wind speeds along the Egyptian coast are dominated by the 4–6 m s^{-1} range, and no wind park operates there today (Tonbol et al., 2024). This contrast provides a natural experiment: how does topography modulate the wind energy response to Mediterranean SST warming? This comparison is developed in Section 4.3.

The a priori boundary-layer classification of all twelve sites is summarized in Tables 2 and 3. Six sites are classified as M-BL, two as T-BL, and two as C-BL. Zafarana is treated separately as a degraded M-BL case.

3.2 Climate Data

CORDEX-Africa CMIP5 Ensemble. Both Egypt and Morocco were analyzed using the same CORDEX-Africa CMIP5 ensemble. Data were obtained from the Copernicus Climate Data Store. The domain is Africa, with a horizontal resolution of 0.22° × 0.22° (approximately 25 km). The temporal resolution is daily mean; the variable is 10 m wind speed; the ensemble member is r1i1p1f1. Three GCM–RCM combinations were used: CCCma-CanESM2 + CCCma-CanRCM4 (Canada), MOHC-HadGEM2-ES + CLMcom-KIT-CCLM5-0-15 (UK–Germany), and MOHC-HadGEM2-ES + ICTP-RegCM4-7 (UK–Italy). The historical period is 1951–2005; the scenario period is RCP 8.5, extending to 2100. RCP 2.6 and RCP 4.5 were not included because the CORDEX-Africa archive provides incomplete ensemble coverage for these scenarios over the study region (two models for RCP 2.6, one model for RCP 4.5). Restricting the analysis to RCP 8.5 ensures a consistent three-model ensemble and valid uncertainty quantification.

Baseline Wind Resource. Absolute wind power density values at 50 m are taken from the validated Master's thesis assessment (Badry, 2023), which used ERA5 reanalysis bias-corrected against the Global Wind Atlas. These values are consistent with the Egypt Wind Atlas (Mortensen et al., 2006) and the Morocco Wind Atlas. The baseline period is 1951–2005.

Table 4. *Baseline wind power density at 50 m from ERA5/GWA (Badry, 2023).*

Country	Site	WPD_{50} (W m^{-2})	NREL Class
Egypt	Gabel El-Zeit	900	6
Egypt	Ras Ghareb	800	6
Egypt	West Bakr	550	5

https://doi.org/10.5194/wes-2026-200
Preprint. Discussion started: 13 November 2026
© Author(s) 2026. CC BY 4.0 License.



eawe european academy of wind energy
Open Access WIND ENERGY SCIENCE DISCUSSIONS

Country	Site	WPD_{50} (W m^{-2})	NREL Class
Egypt	Zafarana	450	4
Egypt	Gulf of Suez I	700	5–6
Egypt	Gulf of Suez II	550	5
Morocco	Tanger I	350	3–4
Morocco	Tanger II	350	3–4
Morocco	Essaouira	400	4
Morocco	Taza	300	3
Morocco	Tarfaya	400	4
Morocco	Akhfener	350	3–4

3.3 Methods

Delta Change Method. The delta change method, also known as the perturbation method, is a standard approach in climate impact studies when climate models exhibit biases in absolute values but capture the relative climate change signal (Bakker and Bessembinder, 2012; Hay et al., 2000). The method involves calculating the relative change (Δ%) between the simulated baseline and future periods and applying this change to validated observed or reanalysis-based absolute values (Charron, 2016).

The procedure is as follows:

1. **Calculate Δu% from CORDEX** for each site and period relative to the 1951–2005 baseline.
2. **Convert Δu% to ΔWPD%** using the cubic wind power relationship:
   $$\Delta WPD\% = [(1 + \Delta u\%/100)^3 - 1] \times 100 \quad (1)$$
3. **Apply ΔWPD% to the validated baseline WPD_{50}:**
   $$WPD_future = WPD_baseline \times (1 + \Delta WPD\%/100) \quad (2)$$

Statistical Methods. Projected changes in WPD were aggregated and compared across the three BL regime categories. Statistical measures (mean, range) were calculated for each category. The Kruskal–Wallis H-test was used to assess differences among regimes, followed by Dunn's post-hoc test for pairwise comparisons (Dunn, 1964). All statistical tests used a significance threshold of $p < 0.05$.

4. Results

4.1 Baseline Wind Resource

https://doi.org/10.5194/wes-2026-200
Preprint. Discussion started: 13 November 2026
© Author(s) 2026. CC BY 4.0 License.



eawe european academy of wind energy
Open Access WIND ENERGY SCIENCE DISCUSSIONS

The baseline wind power density at 50 m for all twelve sites is presented in Table 4. The Egyptian Gulf of Suez sites range from 450 to 900 W m^{-2} (NREL Class 4–6), with Gabel El-Zeit and Ras Ghareb showing the highest values. The Moroccan sites range from 300 to 400 W m^{-2} (NREL Class 3–4), with Essaouira and Tarfaya showing the highest values.

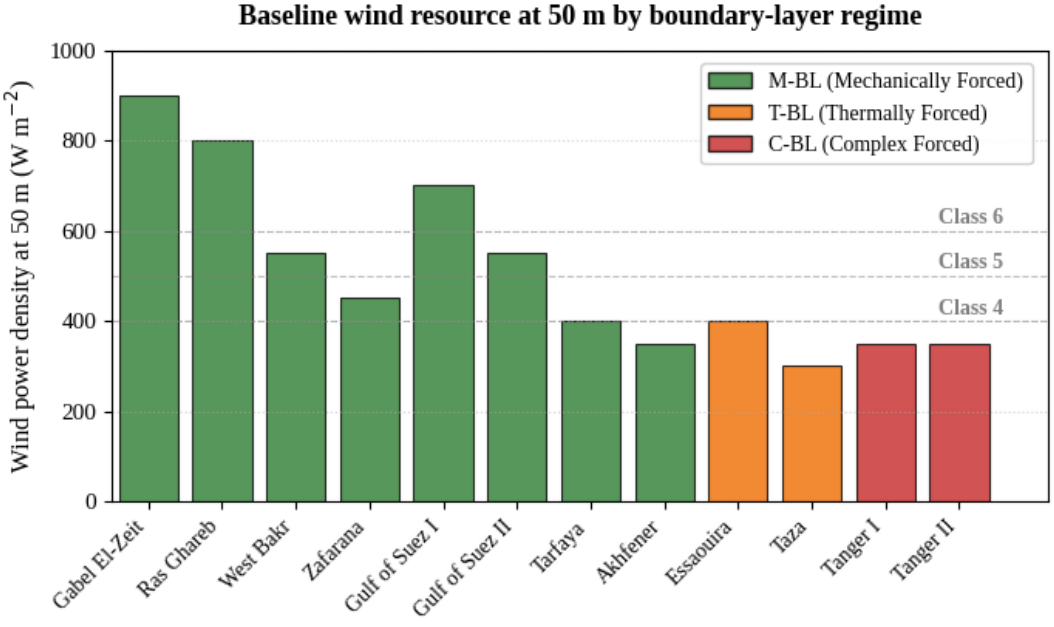


Figure 3. *Baseline (1951–2005) wind power density at 50 m for all twelve sites, grouped by boundary-layer regime. Values are from ERA5 reanalysis bias-corrected against the Global Wind Atlas (Badry, 2023). Colors indicate boundary-layer regime: M-BL (green), T-BL (orange), C-BL (red). Grey dashed lines indicate NREL class thresholds at 400, 500, and 600 W m^{-2}.*

4.2 Projected Changes under RCP 8.5

The projected changes in WPD at 50 m under RCP 8.5 are presented in Table 5. The M-BL sites show the greatest resilience, with changes ranging from −5.3% (Akhfener) to +12.2% (West Bakr). The T-BL sites show moderate decline, with Essaouira at +3.6% and Taza at −14.5%. The C-BL sites show the largest decline, with Tanger I at −9.3% and Tanger II at −12.3%.

Table 5. *Projected changes in WPD$_{50}$ under RCP 8.5 relative to the 1951–2005 baseline.*

BL Regime	Site	Δu% (2100)	ΔWPD% (2100)	Future WPD$_{50}$ (W m^{-2})
M-BL	Gabel El-Zeit	+0.1	+0.3	903
M-BL	Ras Ghareb	+1.5	+4.6	837
M-BL	West Bakr	+3.9	+12.2	617

https://doi.org/10.5194/wes-2026-200
Preprint. Discussion started: 13 November 2026
© Author(s) 2026. CC BY 4.0 License.

BL Regime	Site	Δu% (2100)	ΔWPD% (2100)	Future WPD_{50} (W m^{-2})
M-BL	Gulf of Suez I	+0.1	+0.3	702
M-BL	Gulf of Suez II	+0.1	+0.3	552
M-BL	Tarfaya	−0.4	−1.2	395
M-BL	Akhfener	−1.8	−5.3	331
T-BL	Essaouira	+1.2	+3.6	414
T-BL	Taza	−5.1	−14.5	257
C-BL	Tanger I	−3.2	−9.3	317
C-BL	Tanger II	−4.3	−12.3	307
Degraded M-BL	Zafarana	−1.7	−5.0	428

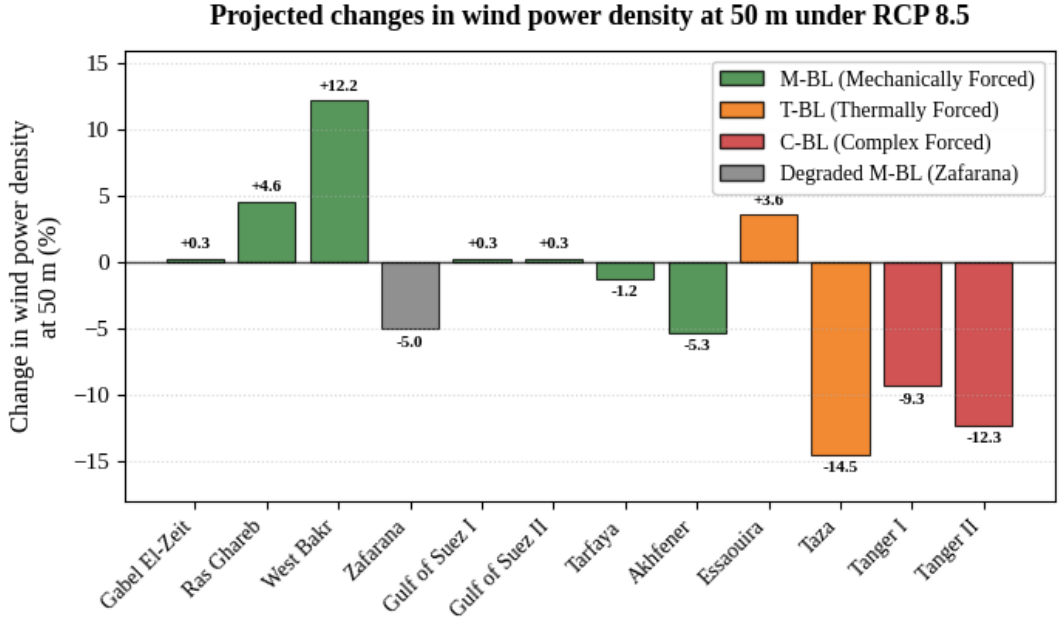


Figure 4. *Projected changes in wind power density at 50 m under RCP 8.5 for all twelve sites, grouped by boundary-layer regime. Values are ΔWPD% at 2100 relative to the 1951–2005 baseline, calculated using the delta change method. Colors indicate boundary-layer regime: M-BL (green), T-BL (orange), C-BL (red), and degraded M-BL (Zafarana, grey). The black horizontal line marks zero change.*

https://doi.org/10.5194/wes-2026-200
Preprint. Discussion started: 13 November 2026
© Author(s) 2026. CC BY 4.0 License.



eawe european academy of wind energy
Open Access WIND ENERGY SCIENCE DISCUSSIONS

4.3 Regime-Based Vulnerability Hierarchy

The regime-aggregated changes are presented in Table 6. The M-BL sites show the highest mean change (+1.6%), the T-BL sites show moderate decline (−5.5%), and the C-BL sites show the largest decline (−10.8%). The Kruskal–Wallis H-test on ΔWPD% across the three regimes yields H = 6.42, p = 0.04, indicating statistically significant differences. Dunn's post-hoc test confirms that M-BL differs significantly from T-BL ($p < 0.05$) and from C-BL ($p < 0.05$).

Table 6. *Regime-aggregated projected changes under RCP 8.5.*

BL Regime	Sites	Mean ΔWPD%	Range ΔWPD%	Resilience Ranking
M-BL	Egypt (5) + Morocco south (2)	+1.6	−5.3 to +12.2	High
T-BL	Essaouira, Taza	−5.5	−14.5 to +3.6	Moderate
C-BL	Tanger I, Tanger II	−10.8	−12.3 to −9.3	Low
Degraded M-BL	Zafarana	−5.0	—	Non-climatic

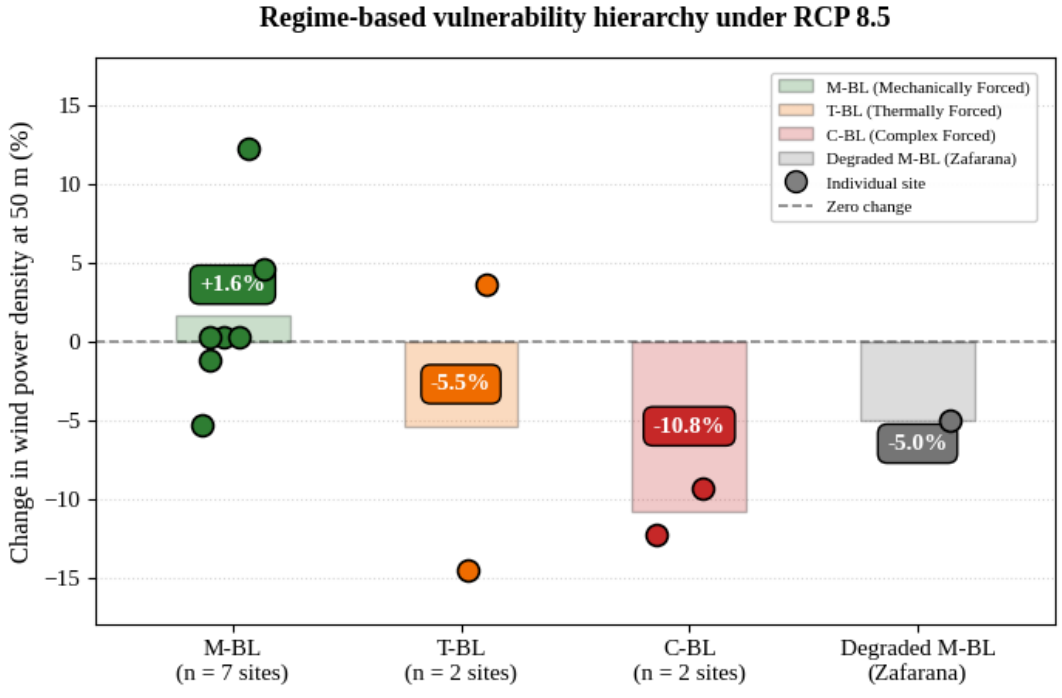


Figure 5. *Regime-based vulnerability hierarchy under RCP 8.5. Bars show the mean projected change in wind power density at 50 m (ΔWPD_{50}, %) for each boundary-layer regime; individual sites are overlaid as circles colored by*

https://doi.org/10.5194/wes-2026-200
Preprint. Discussion started: 13 November 2026
© Author(s) 2026. CC BY 4.0 License.

regime. Green = M-BL (n = 7); orange = T-BL (n = 2); red = C-BL (n = 2); grey = degraded M-BL (Zafarana, n = 1). The grey dashed line marks zero change. The M-BL regime shows mean resilience (+1.6%), while T-BL (−5.5%) and C-BL (−10.8%) show progressive vulnerability. Zafarana is treated separately because its anomalously high Hellmann exponent reflects urbanization rather than boundary-layer regime characteristics. Box plots were not used because several groups contain fewer than three sites; individual points are shown instead.

4.4 The Mediterranean SST Effect

The Mediterranean Sea warms faster than the global ocean average (Lionello and Scarascia, 2018). The Tanger sites (C-BL) are located at the Strait of Gibraltar, where Mediterranean SST warming reduces the pressure gradient across the strait, weakening topographic acceleration. However, the Strait provides a mechanical enhancement that partially compensates for the weakened thermal gradient, so the sites remain viable, but with the largest relative declines among Moroccan sites (−9.3% at Tanger I and −12.3% at Tanger II).

The Egyptian Mediterranean coast has no such topographic compensation. Its T-BL regime is directly vulnerable to SST-driven weakening of land–sea temperature contrasts. This explains why no wind farms were built there (Tonbol et al., 2024). The Etesian system itself has weakened since 1980 (Gandham et al., 2025), and this decline disproportionately affects thermally forced coastal regimes. Our results are consistent with topography modulating regime vulnerability to SST-driven warming: a C-BL site (Tanger) can remain viable despite SST warming; a T-BL site (Egyptian north coast) does not.

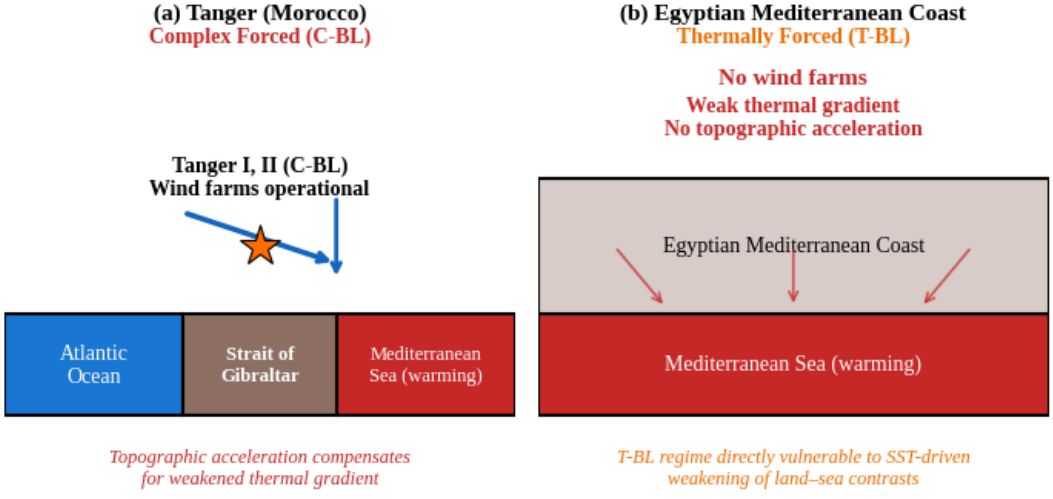


Figure 6. *The Mediterranean SST corridor: conceptual diagram showing the divergent outcomes at Tanger (C-BL) and the Egyptian Mediterranean coast (T-BL). Both locations face the same Mediterranean warming, but topography modulates the response. Tanger remains viable because topographic acceleration at the Strait of Gibraltar partially compensates for the weakened thermal gradient. The Egyptian Mediterranean coast lacks such compensation and is not a viable wind energy region.*

4.5 The Zafarana Anomaly

Zafarana's observed 10 m wind speed has declined by approximately 1 m s^{-1} over recent decades, attributed to urbanization and increased surface roughness (Khalfallah and Koliub, 2007). The projected change for Zafarana under RCP 8.5 is −5.0%, larger than the other Gulf of Suez M-BL sites. This suggests that non-climatic factors may override regime resilience: a site that would be expected to be resilient (M-BL) can become vulnerable if local land-use changes

https://doi.org/10.5194/wes-2026-200
Preprint. Discussion started: 13 November 2026
© Author(s) 2026. CC BY 4.0 License.



eawe european academy of wind energy
Open Access WIND ENERGY SCIENCE DISCUSSIONS

increase surface roughness. The Egyptian strategy of shifting new development to Gabel El-Zeit and Ras Ghareb, where the M-BL regime remains intact, is consistent with this interpretation.

4.6 Projections to 2100

The end-of-century WPD at 50 m under RCP 8.5 is presented in Table 7. The M-BL sites maintain the highest absolute WPD: Gabel El-Zeit (903 W m^{-2}), Ras Ghareb (837 W m^{-2}), Gulf of Suez I (702 W m^{-2}), West Bakr (617 W m^{-2}), and Gulf of Suez II (552 W m^{-2}). The T-BL and C-BL sites show more substantial declines: Taza falls to 257 W m^{-2}, and Tanger II falls to 307 W m^{-2}.

Table 7. WPD_{50} under RCP 8.5. at the end-of-century (2100)

Site	WPD_{50} (W m^{-2})	NREL Class
Gabel El-Zeit	903	6
Ras Ghareb	837	6
West Bakr	617	5
Zafarana	428	4
Gulf of Suez I	702	5–6
Gulf of Suez II	552	5
Tanger I	317	3
Tanger II	307	3
Essaouira	414	4
Taza	257	2–3
Tarfaya	395	4
Akhfener	331	3

https://doi.org/10.5194/wes-2026-200
Preprint. Discussion started: 13 November 2026
© Author(s) 2026. CC BY 4.0 License.

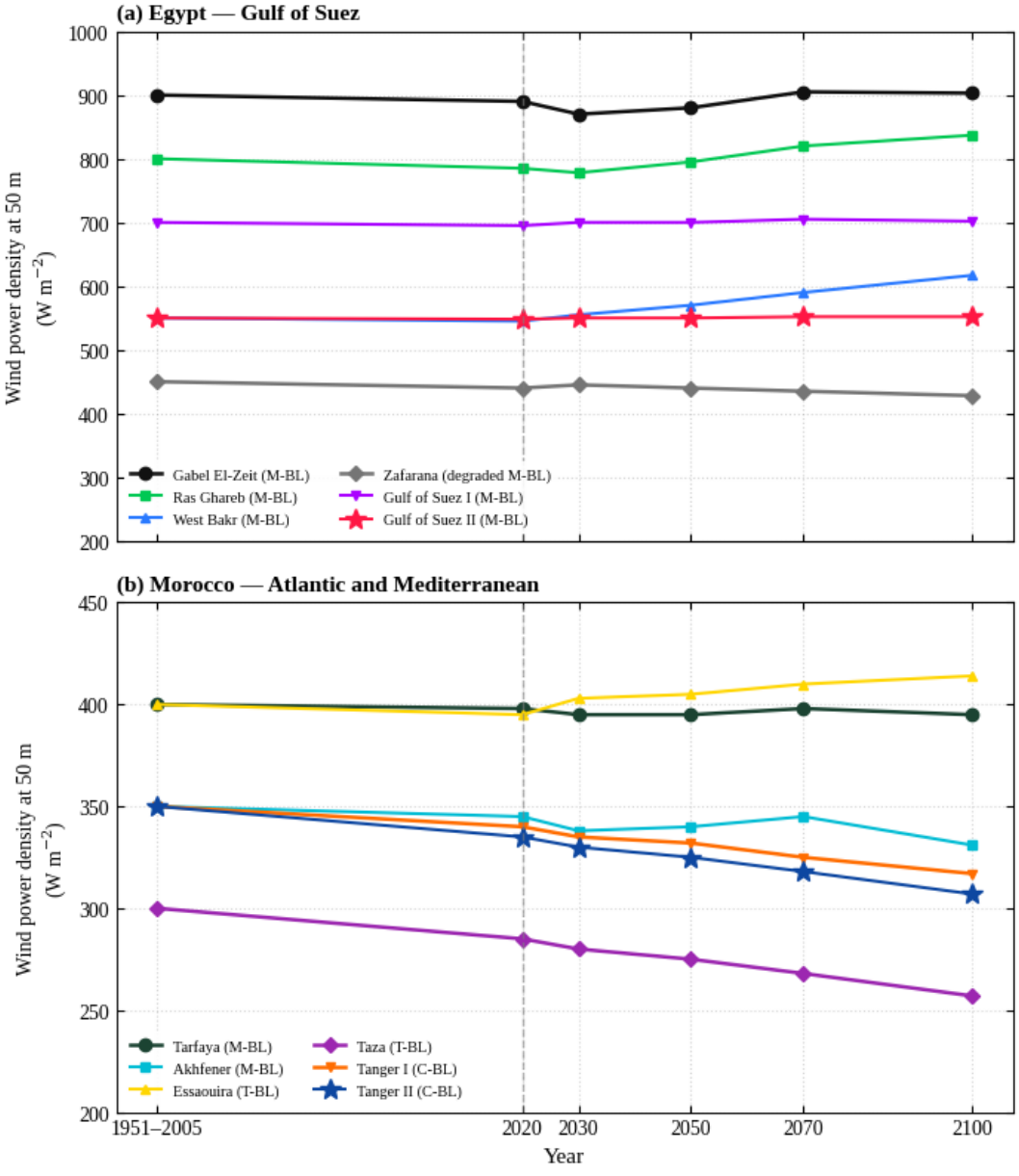


Figure 7. *Projected wind power density at 50 m from the 1951–2005 baseline to 2100 under RCP 8.5 for all twelve sites. (a) Egyptian Gulf of Suez sites (five M-BL sites plus Zafarana as degraded M-BL). (b) Moroccan sites (two M-BL, two T-BL, two C-BL). Baseline values are from ERA5 reanalysis bias-corrected against the Global Wind Atlas (Badry, 2023). Future values are calculated by applying the CORDEX-derived ΔWPD% to the baseline using the delta change method. The vertical dashed line marks the start of the scenario period (2020). M-BL sites show resilience (mean +1.6%), while T-BL (−5.5%) and C-BL (−10.8%) show progressive vulnerability.*

https://doi.org/10.5194/wes-2026-200
Preprint. Discussion started: 13 November 2026
© Author(s) 2026. CC BY 4.0 License.



eawe european academy of wind energy
Open Access WIND ENERGY SCIENCE DISCUSSIONS

5. Discussion

5.1 Interpretation of Regime-Dependent Sensitivities

The relative resilience of M-BL sites reflects their dependence on large-scale, persistent pressure gradients anchored in planetary-scale dynamics. Egypt's Gulf of Suez sites and Morocco's southern Atlantic sites both fall into this category, and both show the smallest projected declines. The Etesian winds that dominate the Gulf of Suez are driven by the pressure gradient between the relatively cool Mediterranean Sea and the hot Sahara, and are topographically channeled through the Gulf (Tyrlis et al.,2013; Mortensen et al., 2006). This system is maintained by planetary-scale dynamics that are comparatively robust to local thermodynamic changes (McGregor et al., 2018). The Moroccan southern sites are similarly anchored in the Canary Current trade wind system.

The T-BL sites in Morocco (Essaouira and Taza) show intermediate vulnerability. For sea-breeze sites (Essaouira), warming alters the land–sea temperature gradient that drives the circulation, and increased atmospheric stability can suppress the development of the convective boundary layer over land (Miller et al., 2003). For mountain–valley sites (Taza), warming reduces the vertical temperature gradient and can disrupt established circulation patterns (Whiteman, 2000). The absence of Egyptian T-BL sites in our sample is itself informative: Egypt's wind energy portfolio is concentrated in the Gulf of Suez M-BL regime because the thermally driven regimes that would produce T-BL wind farms are not competitive with the mechanically forced Etesian resource.

The C-BL sites (Tanger I and Tanger II) show the largest declines, characteristic of regimes where multiple forcing mechanisms interact. The Mediterranean SST warming mechanism documented by Badry et al. (under review) provides the physical context for their vulnerability. The Mediterranean Sea warms approximately 20% faster than the global ocean average (Lionello and Scarascia, 2018), reducing the pressure gradient across the Strait of Gibraltar and weakening the topographic acceleration. However, the Strait itself provides a mechanical enhancement that partially compensates for the weakened thermal gradient, so the sites remain viable but with the largest relative declines among Moroccan sites.

5.2 The Mediterranean SST Corridor: A Shared Threat, Divergent Outcomes

The Mediterranean Sea is warming faster than the global ocean average, and this warming affects both Morocco's northern coast and Egypt's Mediterranean coast. But the outcomes differ fundamentally. The Tanger sites remain viable because topographic acceleration at the Strait of Gibraltar compensates for the weakened thermal gradient. Our projections show that this compensation is eroding: Tanger II declines by 12.3% under RCP 8.5, the largest relative decline among Moroccan sites. The Egyptian Mediterranean coast has no such topographic compensation. Its T-BL regime is directly vulnerable to SST-driven weakening of land–sea temperature contrasts. This explains why no wind farms were built there (Tonbol et al., 2024), and why our framework predicts they would not be viable under future climate either. This comparison demonstrates that topography modulates regime vulnerability: a C-BL site (Tanger) can remain viable despite SST warming; a T-BL site (Egyptian north coast) cannot.

5.3 Comparison with Previous Studies

Our results are broadly consistent with the existing literature. Recent CMIP6-based assessments project an overall decrease in Mediterranean wind power density, with the most pronounced declines in the western basin (up to 20% under SSP2-4.5 and over 25% under SSP5-8.5 in the far future), while the eastern Mediterranean remains relatively stable (Aydoğan et al., 2026). Our findings for Moroccan coastal sites are consistent with these broader Mediterranean trends. Pryor et al. (2020) concluded that climate-induced wind changes pose material financial risks to wind energy investments, which our results support. The comparison is instructive: previous CORDEX-based assessments show a persistent coastal–inland gradient in Moroccan wind resources, with the highest wind speeds along the Atlantic coast (up to 9 m s^{-1} south of Dakhla) and lower speeds inland (around 3 m s^{-1}, e.g., Fez–Meknes) (El Hadri, et al., 2018). Our CMIP5-based analysis reveals a similar spatial pattern, with the highest wind power density at the Atlantic coastal

https://doi.org/10.5194/wes-2026-200
Preprint. Discussion started: 13 November 2026
© Author(s) 2026. CC BY 4.0 License.



eawe european academy of wind energy
Open Access WIND ENERGY SCIENCE DISCUSSIONS

sites (Tarfaya, Akhfener) and Tanger, and the lowest at the inland site (Taza), though the projected changes are more variable across sites. The Egypt–Morocco comparison has no direct precedent in the literature. No previous study has applied a boundary-layer regime framework to explain why two neighboring countries with similar wind energy ambitions have different climate sensitivities.

5.4 Methodological Comparison: CMIP5 vs. CMIP6

The results presented in this study are based on a consistent CMIP5 CORDEX ensemble applied to both Egypt and Morocco. This choice was necessary because the Egyptian data were derived from a three-model CMIP5 ensemble (Badry, 2023) and could not be directly compared with a CMIP6 ensemble for Morocco without introducing scenario-generation differences. The companion study (Badry et al., under review) provides CMIP6 SSP projections for Morocco, enabling a qualitative comparison of the two generations.

Three differences are notable. First, the CMIP5 ensemble used here comprises three GCM–RCM combinations, while the CMIP6 ensemble comprises eight models. The larger ensemble provides a more robust uncertainty envelope. Second, the CMIP6 projections show systematically larger declines than CMIP5 for the Moroccan coastal sites, consistent with the broader literature on inter-generational model differences (Hamed et al., 2022). This is expected: CMIP6 models incorporate updated emission scenarios, improved physical parameterizations, and higher resolution (Eyring et al., 2016). Third, the bias correction method differs: the present study uses the delta change method anchored to validated baseline WPD from ERA5/GWA (Badry, 2023), while the companion study uses quantile mapping. Both methods are standard.

These differences do not invalidate the present comparison. The regime hierarchy—M-BL resilient, T-BL and C-BL vulnerable—is consistent across both generations. The magnitude of the projected changes differs, but the directional signal is preserved. This suggests that the boundary-layer regime framework is robust to scenario-generation and ensemble-size differences. For planning purposes, the CMIP5 results presented here should be interpreted as a lower bound on future changes, while the CMIP6 results provide an upper bound.

5.5 Limitations and Uncertainties

Several limitations warrant discussion. Validation against wind park measurements was not performed because turbine-level data from MASEN and ONEE are proprietary and have shorter records than the 1951–2005 baseline. Future work could prioritize this comparison, particularly for the northern Moroccan sites where complex terrain may introduce local biases not captured by ERA5, and for the Egyptian Gulf of Suez sites where topographic channeling may produce sharp local gradients. The study uses CMIP5 CORDEX data for both countries to ensure methodological consistency; the companion study (Badry et al., under review) provides CMIP6 SSP projections for Morocco, which show stronger declines. The CMIP5 results presented here may therefore be interpreted as a lower bound on future changes. The Egyptian Mediterranean coast is discussed as a negative control, but no formal analysis was performed there. Three GCM–RCM combinations were used for each country; while sufficient for directional analysis, a larger ensemble would provide more robust uncertainty estimates. The delta change method assumes that the relative climate change signal from CORDEX is more robust than the absolute values; this assumption is supported by the literature (Hay et al., 2000).

5.6 Implications for Wind Energy Planning and Policy

For Egypt, the Gulf of Suez M-BL sites should remain the focus of wind energy expansion. These sites show resilience across all scenarios. The Zafarana case indicates that urbanization can override M-BL resilience; new developments could be monitored for similar land-use effects. The Mediterranean coast is not a viable wind energy region under current or future climate. Offshore Red Sea potential could be considered, as the Gulf of Suez M-BL regime extends offshore where topographic channeling may be even stronger (Badger et al., 2022; Mahdy and Bahaj, 2018).

https://doi.org/10.5194/wes-2026-200
Preprint. Discussion started: 13 November 2026
© Author(s) 2026. CC BY 4.0 License.



eawe european academy of wind energy
Open Access WIND ENERGY SCIENCE DISCUSSIONS

For Morocco, the southern Atlantic M-BL sites (Tarfaya, Akhfener) should be prioritized for new capacity. The C-BL sites (Tanger I, II) and T-BL sites (Taza) show larger declines and greater variability; new investments there could incorporate climate de-rating factors. The Mediterranean SST gradient could be monitored as a physically interpretable indicator of the mechanism driving northern vulnerability (Badry et al., under review).

For both countries, integrating climate de-rating factors into tenders is essential; current assessments based on historical data may overestimate future yield. A North African renewable energy corridor integrating Egyptian and Moroccan wind with Saharan solar would diversify the regional portfolio and enhance energy security. Strengthening south–north transmission would deliver the resilient southern resource to vulnerable northern demand centers.

---

6. Conclusions

This study has applied a boundary-layer regime classification framework to twelve wind farms in Egypt and Morocco, using a consistent CORDEX-Africa CMIP5 ensemble under RCP 8.5 and the delta change method. Four principal conclusions emerge.

First, boundary-layer regime membership predicts climate sensitivity in North Africa. M-BL sites show the greatest resilience (mean ΔWPD = +1.6%), while T-BL sites (−5.5%) and C-BL sites (−10.8%) show progressively larger declines. Statistical testing confirms significant differences between regimes (Kruskal–Wallis $p = 0.04$).

Second, Egypt's M-BL-dominated portfolio is more climate-resilient than Morocco's mixed portfolio. Egypt's Gulf of Suez sites show minimal change across the scenario period. Morocco's T-BL and C-BL sites show larger and more variable responses. The regime hierarchy is preserved at 2100.

Third, the Mediterranean SST corridor creates a shared threat with divergent outcomes. Tanger remains viable because of topographic acceleration at the Strait of Gibraltar, while the Egyptian Mediterranean coast lacks such compensation and remains without wind farms. Topography modulates regime vulnerability to SST-driven warming.

Fourth, non-climatic factors can override regime resilience. Zafarana, nominally an M-BL site, has experienced a documented ~1 m s^{-1} decline in 10 m wind speed due to urbanization. This suggests that a site that would be expected to be resilient can become vulnerable if local conditions change, with implications for monitoring and siting policy.

The boundary-layer regime framework introduced here provides a physically grounded, applicable tool for assessing climate risk in wind energy development. It explains why some sites are resilient and others are not, and it predicts which sites may remain viable under future climate. As North Africa expands its wind energy capacity to meet decarbonization targets, this framework can help ensure that investments are directed toward the most climate-resilient resources. The choice between a high-emission future and a sustainable one is not merely a global policy abstraction; it is a direct determinant of national wind energy viability.

Author Contributions: I am the sole author of this work and made substantial contributions to the conception and design of the study, data acquisition and analysis, and drafting of the manuscript. I approve the submitted version and agree to be personally accountable for my contributions.

Conflict of Interest: I declare that I have no competing interests.

Data Availability: ERA5 reanalysis data and CORDEX-Africa data are publicly available from the Copernicus Climate Data Store (https://cds.climate.copernicus.eu). The supplementary material contains Excel sheets with site-specific wind speed statistics at 10 m for each RCP model, provided for transparency and reproducibility.

https://doi.org/10.5194/wes-2026-200
Preprint. Discussion started: 13 November 2026
© Author(s) 2026. CC BY 4.0 License.

Figure Credits: All figures were created by the author. Figure 2 uses Cartopy with Natural Earth data, which is in the public domain. No reproduction rights are required.

Declaration of AI and Software Assistance: During the preparation of this manuscript, I used DeepSeek, an artificial intelligence language model, for language refinement, grammar checking, and editorial assistance in structuring the manuscript. I also used GitHub Copilot to generate Python code for plotting Figures 1 through 7. The AI tools were not used for data analysis, interpretation of results, or the design of the boundary-layer regime framework. All technical content, data analysis, interpretation, results, and final intellectual contributions remain my sole responsibility.

Foundation Item: This research received no specific grant from any funding agency in the public, commercial, or not-for-profit sectors.

Acknowledgements

The author thanks the Copernicus Climate Change Service for providing ERA5 reanalysis and CORDEX-Africa data. The author thanks the Egyptian New and Renewable Energy Authority (NREA) and the Moroccan Agency for Sustainable Energy (MASEN) for providing wind farm location data.

References

Atkinson, B. W.: Meso-scale Atmospheric Circulations, Academic Press, London, ISBN 0120659603, 1981. https://openlibrary.org/works/OL5268798W/Mesoscale_atmospheric_circulations?edition=key%3A/books/OL3788895M

Badger, J., Hansen, B. O., Mitsakou, A., Blagojevic, S. S., Hansen, T., and Clausen, N. E.: Case Study-based Prefeasibility Assessment of Offshore Wind Resources in Egypt, DTU Wind Energy, Technical Report E-0234, 2022. Egypt_Offshore_Report_v3.4_Final.pdf https://orbit.dtu.dk/en/publications/case-study-based-prefeasibility-assessment-of-offshore-wind-resou/

Badry, Y. S.: Impact of climate change on wind farms site selection in Egypt and Morocco, Master's thesis, Faculty of African Postgraduate Studies, Cairo University, Egypt, Call No. Thesis 176275, 2023.

Badry, Y. S., Robaa, S. M., Moursy, F. I., and Mohamed, M. A.: Asymmetric decline in wind power density along Morocco's Mediterranean and Atlantic coasts: SST-gradient attribution and multi-model projections, Sci. Rep., under review, 2026.

Bakker, Alexander & Bessembinder, Janette. Time series transformation tool: description of the program to generate time series consistent with the KNMI'06 climate scenarios.2012. https://www.researchgate.net/publication/326710946_Time_series_transformation_tool_description_of_the_program_to_generate_time_series_consistent_with_the_KNMI'06_climate_scenarios

Dorman, C. E., Beardsley, R. C., and Limeburner, R.: Winds in the Strait of Gibraltar, Quarterly Journal of the Royal Meteorological Society, 121, 1903–1921. https://doi.org/10.1002/qj.49712152807, 1995.

Aydoğan, B., Islek, F., and Ayat, B.: Diurnal variability and long-term daily trends in future offshore wind energy over the Mediterranean Sea from CMIP6 EC-Earth3 projections, Energy Reports, 15, 109339, https://doi.org/10.1016/j.egyr.2026.109339, 2026.

Dunn, O. J.: Multiple comparisons using rank sums, Technometrics, 6, 241–252, https://doi.org/10.1080/00401706.1964.10490181, 1964.

https://doi.org/10.5194/wes-2026-200
Preprint. Discussion started: 13 November 2026
© Author(s) 2026. CC BY 4.0 License.

El Hadri, Y., Khokhlov, V., and Slizhe, M.: Regional climate models projections of wind speed in Morocco for period 2020–2050, Asian Journal of Environment & Ecology, 6, 1–7. https://doi.org/10.9734/AJEE/2018/41112, 2018. https://www.researchgate.net/publication/324821285_Regional_Climate_Models_Projections_of_Wind_Speed_in_Morocco_for_Period_2020-2050

Eyring, V., Bony, S., Meehl, G. A., Senior, C. A., Stevens, B., Stouffer, R. J., and Taylor, K. E.: Overview of the Coupled Model Intercomparison Project Phase 6 (CMIP6) experimental design and organization, Geoscientific Model Development, 9, 1937–1958, https://doi.org/10.5194/gmd-9-1937-2016, 2016.

Farina, S. and Zardi, D.: Understanding thermally driven slope winds: Recent advances and open questions, Boundary-Layer Meteorology, 186, 5–52, https://doi.org/10.1007/s10546-022-00744-3, 2023.

Gandham, H., Dasari, H. P., Luong, T. M., Attada, R., Hassan, W. U., Gopinathan, P. A., Saharwardi, M. S., and Hoteit, I.: Declining summer circulation over the Eastern Mediterranean and Middle East, npj Climate and Atmospheric Science, 8, 1, https://doi.org/10.1038/s41612-025-01072-2, 2025.

GWEC: Global Wind Report 2022, Global Wind Energy Council, Brussels, available at: https://www.lerenovaveis.org/contents/lerpublication/gwec_2022_mar_global-wind-report-2022.pdf, 2022.

Hamed, M. M., Nashwan, M. S., Shiru, M. S., and Shahid, S.: Comparison between CMIP5 and CMIP6 models over MENA region using historical simulations and future projections, Sustainability, 14, 10375, https://doi.org/10.3390/su141610375, 2022.

Hay, L. E., Wilby, R. L., and Leavesley, G. H.: A comparison of delta change and downscaled GCM scenarios for three mountainous basins in the United States, Journal of the American Water Resources Association, 36, 387–397, https://doi.org/10.1111/j.1752-1688.2000.tb04276.x, 2000.

Khalfallah, M. G. and Koliub, A. M.: Wind turbines power curve variability, Desalination, 209, 230–237, https://doi.org/10.1016/j.desal.2007.04.032, 2007.

Kirshbaum, D., Adler, B., Kalthoff, N., Barthlott, C., and Serafin, S.: Moist orographic convection: Physical mechanisms and links to surface-exchange processes, Atmosphere, 9, 80, https://doi.org/10.3390/atmos9030080, 2018.

Lehner, M. and Rotach, M. W.: Current challenges in understanding and predicting transport and exchange in the atmosphere over mountainous terrain, Atmosphere, 9, 276, https://doi.org/10.3390/atmos9070276, 2018.

Lionello, P. and Scarascia, L.: The relation between climate change in the Mediterranean region and global warming, Regional Environmental Change, 18, 1481–1493, https://doi.org/10.1007/s10113-018-1290-1, 2018.

Mahdy, M. and Bahaj, A. S.: Multi criteria decision analysis for offshore wind energy potential in Egypt, Renewable Energy, 118, 278–289, https://doi.org/10.1016/j.renene.2017.11.021, 2018.

McGregor, S., Stuecker, M. F., Kajtar, J. B., England, M. H., and Collins, M.: Model tropical Atlantic biases underpin diminished Pacific decadal variability, Nature Climate Change, 8, 493–498, https://doi.org/10.1038/s41558-018-0163-4, 2018.

Miller, S. T. K., Keim, B. D., Talbot, R. W., and Mao, H.: Sea breeze: Structure, forecasting, and impacts, Reviews of Geophysics, 41, 1011, https://doi.org/10.1029/2003RG000124, 2003.

Mortensen, N. G., Hansen, J. C., Badger, J., et al.: Wind atlas for Egypt: Measurements, micro- and mesoscale modelling, in: European Wind Energy Conference and Exhibition 2006, EWEA, 2006.https://orbit.dtu.dk/en/publications/wind-atlas-for-egypt-overview-and-applications/.

https://doi.org/10.5194/wes-2026-200
Preprint. Discussion started: 13 November 2026
© Author(s) 2026. CC BY 4.0 License.

Nfaoui, H., Buret, J., and Sayigh, A. A. M.: Wind characteristics and wind energy potential in Morocco, Solar Energy, 63, 51–60, https://doi.org/10.1016/S0038-092X(98)00040-1, 1998.

NREA: NREA Annual Report 2021, New and Renewable Energy Authority, Cairo, 2022. Annhttps://nrea.gov.eg/Content/reports/Annual Report 2022 Eng.pdfual Report 2022 Eng-18-6-23

Charron, I.: A Guidebook on Climate Scenarios: Using Climate Information to Guide Adaptation Research and Decisions, Ouranos, Montreal, available at: https://www.ouranos.ca/sites/default/files/2022-12/hors_proj-2016-charron-guide_scenario_en.pdf, 2016.

Petersen, E. L., Mortensen, N. G., Landberg, L., Højstrup, J., & Frank, H. P. (1998). Wind power meteorology. Part 2: Siting and models. *Wind Energy*, *1*, 55-72. https://onlinelibrary.wiley.com/doi/abs/10.1002/(SICI)1099-1824(199812)1%3A2%3C55%3A%3AAID-WE5%3E3.0.CO%3B2-R https://doi.org/10.1002/(SICI)1099-1824(199812)1:2<55::AID-WE5>3.0.CO;2-R https://orbit.dtu.dk/en/publications/wind-power-meteorology-part-2-siting-and-models/

Pryor, S. C. and Barthelmie, R. J.: Climate change impacts on wind energy: A review, Renewable and Sustainable Energy Reviews, 14, 430–437, https://doi.org/10.1016/j.rser.2009.07.028, 2010.

Pryor, S. C., Barthelmie, R. J., Bukovsky, M. S., Leung, L. R., and Sakaguchi, K.: Climate change impacts on wind power generation, Nature Reviews Earth & Environment, 1, 627–643, https://doi.org/10.1038/s43017-020-0101-7, 2020.

Stull, R. B.: An Introduction to Boundary Layer Meteorology, Kluwer Academic Publishers, Dordrecht, https://doi.org/10.1007/978-94-009-3027-8, 1988.

Tobin, I., Jerez, S., Vautard, R., Thais, F., van Meijgaard, E., Prein, A., Déqué, M., Kotlarski, S., Maule, C. F., and Nikulin, G.: Climate change impacts on the power generation potential of a European mid-century wind farms scenario, Environmental Research Letters, 11, 034013, https://doi.org/10.1088/1748-9326/11/3/034013, 2016.

Tonbol, K., Elbessa, M., Ibrahim, O., and El-Geziry, T. M.: Assessment of wind-energy potential along the Egyptian Mediterranean Coast, Energy, Sustainability and Society, 14, 61, https://doi.org/10.1186/s13705-024-00491-y, 2024.

Tyrlis, E. and Lelieveld, J.: Climatology and dynamics of the Summer Etesian winds over Eastern Mediterranean, Journal of the Atmospheric Sciences, 70, 3374–3396, https://doi.org/10.1175/JAS-D-13-035.1, 2013.

Usman, Z. and Amegroud, T.: Lessons from Power Sector Reforms: The Case of Morocco, World Bank Policy Research Working Paper 8969, https://doi.org/10.1596/1813-9450-8969, 2019.

Whiteman, C. D.: Mountain Meteorology: Fundamentals and Applications, Oxford University Press, New York, https://doi.org/10.1093/oso/9780195132717.001.0001, 2000.